

Gadolinium Doped Europium Sulfide

Srotoswini Kar,[†] William L. Boncher,[†] Daniel Olszewski,[†] Norman Dollahon,[‡] Richard Ash,[§] and Sarah L. Stoll^{*†}

Department of Chemistry, Box 571227, Georgetown University, Washington D.C. 20057, Department of Biology, Villanova University, Villanova, Pennsylvania 19085, and Department of Geology, University of Maryland, College Park, Maryland 20742

Received June 1, 2010; E-mail: sls55@georgetown.edu

Abstract: We have prepared gadolinium doped europium sulfides, $\text{Eu}_{1-x}\text{Gd}_x\text{S}$ for a doping range of $0 \leq x \leq 0.1$ by thermal decomposition of the precursors $\text{Eu}(\text{S}_2\text{CNET}_2)_3\text{Phen}$ / $\text{Gd}(\text{S}_2\text{CNET}_2)_3\text{Phen}$ with respective ratios. Electron doping provides indirect evidence for the magnetic coupling through carrier electrons in magnetic semiconductors. Based on the magnetic properties, we determined that the paramagnetic Curie temperature, Θ_p , varies with doping level, in a similar way to $\text{Eu}_{1-x}\text{Gd}_x\text{O}$ exhibiting a significant increase at low doping levels. All materials have been characterized by X-ray powder diffraction, magnetic measurements, ICP-MS, and TEM.

There has been significant interest in the synthesis of nanostructures of EuO^1 and EuS^2 in the search for luminescent,³ magnetic,⁴ magnetocaloric,⁵ and photomagnetic properties.⁶ The europium monochalcogenides belong to a rare class of intrinsically magnetic and semiconducting materials and exhibit highly coupled magnetic, electronic, and optical properties.⁷ Within the chalcogenides, the series exhibit the gamut of magnetic ordering from ferromagnetism (EuO $T_c = 66.8$ K, EuS $T_c = 16.6$ K) to antiferromagnetism (EuTe $T_N = 9.64$ K) and metamagnetism (EuSe , antiferromagnetic $T_N = 4.6$ K becomes ferromagnetic at fields >10 KOe).^{8,9} Because of magnetic spin splitting of the conduction band, the band gap in europium chalcogenides decreases with decreasing temperature or increasing applied magnetic field.¹⁰ Magneto-optic effects such as large Faraday^{6b} and Kerr effects have been well studied in these materials.¹¹ Recently thin films of EuO and EuS have been used as spin filters in tunnel junctions.¹²

One of the successful methods for probing the magnetic exchange interactions in europium chalcogenides is electron doping, that is replacing $\text{Eu}(\text{II})$ with one of the nonredox active lanthanides, $\text{Ln}(\text{III})$, resulting in $\text{Eu}^{2+}_{1-x}(\text{Ln}^{3+} + e^-)_x\text{O}$.¹³ Electron doping in single crystals of europium chalcogenides has been shown to introduce free carriers into the conduction band causing a change from semiconducting to metallic properties.^{13a} For small values of 'x' there is a strong increase in T_c proportional to the concentration of 'impurity electrons'. However, the increase in T_c is limited, as the exchange interaction of the conduction electrons should decrease with increasing electron concentration.¹⁴

The most thoroughly studied example is Gd doped EuO . The magnetic ordering in Gd doped EuO has been investigated using reflectivity,¹⁴ NMR line shape,¹⁵ soft X-ray magnetic circular dichroism,¹⁶ Raman scattering,¹⁷ and magnetic and electronic

transport studies.¹⁸ These measurements provide a consistent description of the magnetic properties. The increase in T_c at low doping levels provides indirect evidence for the dependence of the magnetic interaction on carrier electron concentration in these magnetic semiconductors.¹⁹ The drop in T_c at modest gadolinium doping levels is thought to be due to a transition to either a long-range spiral magnetic order or short-range canted domains around Gd impurities.²⁰ The gadolinium doped EuO has also attracted interest due to the discovery of the colossal magnetoresistance effect (CMR) much larger than the manganates, and a system of potential interest for spintronics.²¹ This effect has also been observed in EuSe , where gadolinium doping causes a giant negative magnetoresistance effect.²² Although $\text{Eu}_{1-x}\text{Gd}_x\text{S}$ was reported to be 'qualitatively similar'^{13a} to $\text{Eu}_{1-x}\text{Gd}_x\text{O}$ and $\text{Eu}_{1-x}\text{Gd}_x\text{Se}$, very little data are available on this system and there are no reports on nanostructured systems.

To study the properties of $\text{Eu}_{1-x}\text{Gd}_x\text{S}$ we prepared polycrystalline powders by thermal decomposition in sealed tubes at 700 °C of dithiocarbamate precursors ($\text{Eu}(\text{S}_2\text{CNET}_2)_3\text{Phen}$, $\text{Gd}(\text{S}_2\text{CNET}_2)_3\text{Phen}$) with ratios to give doping levels $x = 0.003$ – 0.1 (see Supporting Information for experimental details). The use of molecular precursors has the advantage that the concentration of Gd can be controlled carefully and homogeneity is improved by dissolving precursors in solution for intimate mixing before thermolysis. For all doping levels, the X-ray powder diffraction patterns indexed to the monosulfide, EuS (see Supporting Information S1),²³ with no evidence of secondary phases particularly $\gamma\text{-Gd}_2\text{S}_3$, which we have found to be the thermolysis product of pure $\text{Gd}(\text{S}_2\text{CN}^i\text{Bu}_2)_3\text{Phen}$. We did not see shifts in lattice parameters according to Vegard's law, presumably due to the close match in lattice constants for EuS (5.97 Å) and GdS (5.55 Å).²⁴ Transmission electron microscopy indicates that the powders have no distinct morphology and are polycrystalline (Supporting Information S2). EDS (S3) was performed on each sample and qualitatively confirmed the presence of Gd; however the close overlap of the lines (for example the K_α for Gd and Eu is 42.992 and 41.543 KeV, respectively) limited more detailed analysis. Therefore we used ICP-MS to measure the Eu–Gd ratio and found that, for all compositions, the actual doping level of Gd was lower than expected (see Supporting Information, Table 1).

The magnetic properties were characterized by measuring the magnetization as a function of temperature (5 – 100 K) for several applied fields (500 – 5000 Oe). The reduced magnetization curves for the low-doped samples $\text{Eu}_{1-x}\text{Gd}_x\text{S}$ ($0 < x < 0.1$) show that the variation of T_c with doping level is quite small (see S4). We have previously used Arrott plots to determine more precisely T_c ;^{4a,b} however, in $\text{Eu}_{1-x}\text{Gd}_x\text{O}$, the reduced magnetization versus temperature plots significantly deviates from Brillouin's law near T_c ,^{25,26} which is a condition for Arrott plots.²⁷ We found, using simple

[†] Georgetown University.

[‡] Villanova University.

[§] University of Maryland.

$1/\chi$ versus temperature plots to determine the paramagnetic Curie temperature, that θ varies systematically with doping level in $\text{Eu}_{1-x}\text{Gd}_x\text{S}$. Here, we report the theta versus x graph for our Gd doped materials in Figure 1. Our graph has the same characteristics as those described in the literature for $\text{Eu}_{1-x}\text{Gd}_x\text{O}$, $\text{Eu}_{1-x}\text{Gd}_x\text{Se}$, and $\text{Eu}_{1-x}\text{Gd}_x\text{Te}$, with a sharp increase at low doping levels as described below. For EuS, the paramagnetic θ is predicted to sharply increase until $x \approx 0.1$ ²⁸ and decrease above this value. For our polycrystalline samples, we found that the θ sharply increased at low doping levels and dropped for high doping levels. Thus although the maximum change in θ was smaller than previously observed, the functional relationship appears to be quite similar.

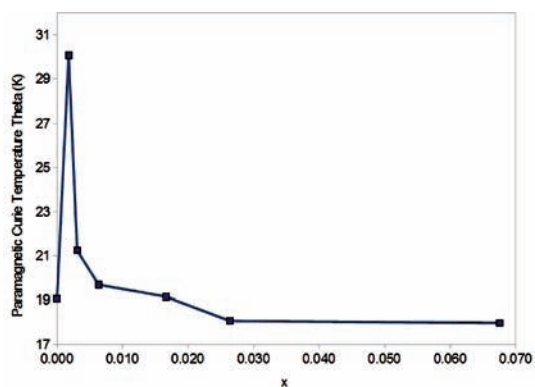


Figure 1. Paramagnetic Curie temperature (θ , K) versus doping level, x , for $\text{Eu}_{1-x}\text{Gd}_x\text{S}$.

Previous work using magnetic susceptibility measurements to characterize the magnetic properties of $\text{Eu}_{1-x}\text{Gd}_x\text{O}$ indicate that the paramagnetic Curie temperature, θ , is larger than T_c (for undoped EuO: $\theta = 79$ K, $T_c = 69.3$ K),²⁹ is more sensitive, and follows a similar trend to that of T_c .^{13a} In addition, the θ allows for a more direct comparison of magnetic coupling between electron doped ferromagnets EuO and EuS and the antiferromagnets EuSe and EuTe.

Analogously, for the doped europium selenides, $\text{Eu}_{1-x}\text{Gd}_x\text{Se}$ and $\text{Eu}_{1-x}\text{La}_x\text{Se}$, the same trend in θ is observed. For Gd doped EuSe, initially θ increases very rapidly from 20 K to a maximum of ~ 45 K at $x \approx 0.1$ and then rapidly decreases to negative values below $x = 0.6$ to $\theta = -60$ K. In contrast to $\text{Eu}_{1-x}\text{Gd}_x\text{O}$, which has a relatively sharp peak in T_c versus x (0.005–0.15), there is a relatively broad range of x (0.002–0.05) in $\text{Eu}_{1-x}\text{Gd}_x\text{Se}$ with increased T_c . In addition, solid solutions have been demonstrated for the full range of $x = 0-1$, and the magnetic properties of highly doped $\text{Eu}_{1-x}\text{Gd}_x\text{Se}$ appear to be closer to a modification of GdSe ($T_N \approx 50$ K, with a negative theta, $\theta = -60$ K).^{13b} Similarly, $\text{Eu}_{1-x}\text{Gd}_x\text{Te}$ also exhibits an increase in the paramagnetic Curie temperature from -10 K to a maximum of $+28$ K.^{13a} Based on these examples, the maximum increase in θ appears to be approximately twice the θ for the undoped material, which for EuS should be ~ 38 K, larger than the 30 K observed here. Furthermore, the range of dopant for which θ increases is narrow as observed in EuO.

One explanation for the low change in θ is that the morphology is important for the magnetic properties. One approach to elucidate this effect is to measure the magnetism for larger and smaller crystallites. We have attempted annealing to increase crystallite size, but even under our controlled conditions this appears to result in oxidation rather than crystallite growth. Therefore, we sought to reduce the crystallite size by preparing nanoparticles for comparison to the polycrystalline samples with the same doping level. Dithio-

carbamate precursors (with a target composition of $\text{Eu}_{0.975}\text{Gd}_{0.025}\text{S}$) were dissolved in a mixture of oleylamine and triphenyl phosphine and heated to 265 °C for 1 h (see Supporting Information for the experimental details). The composition based on ICP-MS was found to be $\text{Eu}_{0.982}\text{Gd}_{0.018}\text{S}$.

The nanoparticles appeared to have a cubic morphology, as we have seen for nanoparticles >10 nm. A representative TEM image is shown in Figure 2b (inset), which was found to have an average

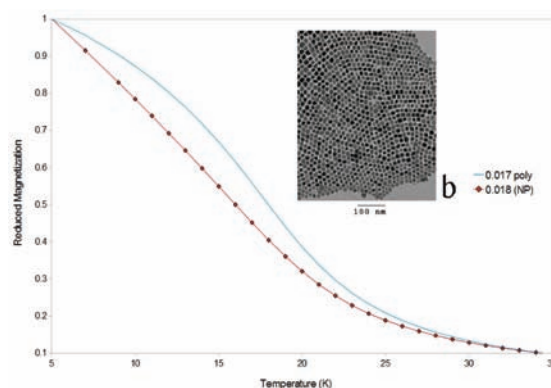


Figure 2. Reduced magnetization of $\text{Eu}_{0.983}\text{Gd}_{0.017}\text{S}$ polycrystalline (solid line), $\text{Eu}_{0.982}\text{Gd}_{0.018}\text{S}$ nanoparticles (squares); inset is the TEM image of the nanoparticles.

particle size of $16.7 (\pm 4.4)$ nm for measurements of ~ 100 individual crystallites.

The reduced magnetization versus temperature plot for the nanoparticles and polycrystalline sample with the closest composition are shown in Figure 2. The θ measured for the $\text{Eu}_{0.98}\text{Gd}_{0.02}\text{S}$ nanoparticles, 5.58 K ($R^2 = 0.9992$), was significantly lower than that found for the $\text{Eu}_{0.983}\text{Gd}_{0.017}\text{S}$ polycrystalline sample where $\theta = 19.4$ K ($R^2 = 1.0000$). This suggests that the reduced crystallite size reduces the paramagnetic Curie temperature. From comparison of the nanoparticles, EuS, $\text{Eu}_{0.99}\text{Gd}_{0.01}\text{S}$, and $\text{Eu}_{0.98}\text{Gd}_{0.02}\text{S}$, the θ was determined to decrease from 17.63 to 7.82 to 5.85 K, respectively.

In summary, using molecular precursors we have prepared a series of electron doped $\text{Eu}_{1-x}\text{Gd}_x\text{S}$ and found that the paramagnetic Curie temperature increases at very low doping levels, as found for EuO, EuSe, and EuTe. The increase is less than expected; however, morphology and crystallite size clearly play a role in the magnetic properties of this system.

Acknowledgment. We thank the National Science Foundation for funding this work (CAREER: 0449829) and George Washington University for aid in obtaining the magnetic measurements.

Supporting Information Available: Experimental details as well as characterization (X-ray powder diffraction, TEM, EDS, ICP-MS, χ versus T , $1/\chi$ versus T) can be found in the Supporting Information. This material is available free of charge via the Internet at <http://pubs.acs.org>.

References

- (1) (a) Hasegawa, Y.; Thongchant, S.; Wada, Y.; Tanaka, H.; Kawai, T.; Sakata, T.; Mori, H.; Yanagida, S. *Angew. Chem., Int. Ed.* **2002**, *41* (12), 2073. (b) Hasegawa, Y.; Thongchant, S.; Kataoka, T.; Wada, Y.; Yatsuhashi, T.; Nakashima, N.; Yanagida, S. *Chem. Lett.* **2003**, *32* (8), 706–709. (c) Bierman, M. J.; Van Heuvelen, K. M.; Schmeiser, D.; Brunold, T. C.; Jin, S. *Adv. Mater.* **2007**, *19*, 2677.
- (2) (a) Thongchant, S.; Hasegawa, Y.; Wada, Y.; Yanagida, S. *J. Phys. Chem. B* **2003**, *107*, 2193. (b) Regulacio, M. D.; Tomson, N.; Stoll, S. L. *Chem. Mater.* **2005**, *17* (12), 3114–3121. (c) Mirkovic, T.; Hines, M.; Nair, P.; Scholes, G. *Chem. Mater.* **2005**, *17*, 3451. (d) Zhao, F.; Sun, H.-L.; Su, G.; Gao, S. *Small* **2006**, *2* (2), 244. (e) Hasegawa, Y.; Afzaal, M.; O'Brien, P.; Waada, Y.; Yanagida, S. *Chem. Commun.* **2005**, *2*, 242.

- (3) (a) Hasegawa, Y.; Okada, Y.; Kataoka, T.; Sakata, T.; Mori, H.; Wada, Y. *J. Phys. Chem. B* **2006**, *110* (18), 9008. (b) Redigolo, M.; Koktysh, D.; van Benthem, K.; Rosenthal, S.; Dickerson, J. *Mater. Chem. Phys.* **2009**, *115* (2–3), 526–529.
- (4) (a) Regulacio, M. D.; Lewis, B.; Bussman, K.; Stoll, S. L. *J. Am. Chem. Soc.* **2006**, *128*, 11173. (b) Regulacio, M. D.; Kar, S.; Zuniga, E.; Wang, G.; Dollahon, N. R.; Yee, G.; Stoll, S. L. *Chem. Mater.* **2008**, 3368. (c) Thongchant, S.; Hasegawa, Y.; Wada, Y.; Yanagida, S. *Chem. Lett.* **2001**, *12*, 1274.
- (5) Ahn, K.; Pecharsky, A. O.; Gschneidner, A. A.; Pecharsky, V. K. *J. Appl. Phys.* **2004**, *97*, 063901.
- (6) (a) Hasegawa, Y.; Thongchant, S.; Wada, Y.; Tanaka, H.; Kawai, T.; Sakata, T.; Mori, H.; Yanagida, S. *Angew. Chem., Int. Ed.* **2002**, *41* (12), 2073–2075. (b) Thongchant, S.; Hasegawa, Y.; Tanaka, K.; Fujita, K.; Hirao, K.; Wada, Y.; Yanagida, S. *Jpn. J. Appl. Phys. Part 2: Lett.* **2003**, *42* (7B), L876.
- (7) Wachter, P. *CRC Crit. Rev. Solid State Sci.* **1972**, *3*, 189.
- (8) Wernick, J. H. *Treatise on Solid State Chemistry, the Chemical Structure of Solids*; Hannay, N. B., Ed.; Plenum Press: New York, 1974; Vol. 1, pp 175–272.
- (9) Fujiwara, H.; Kadomatsu, H.; Kurisu, M.; Hihara, T.; Kojima, K.; Kamigaichi, T. *Solid State Commun.* **1982**, *42*, 509.
- (10) Busch, G.; Wachter, P. *Phys. Kondens. Mater.* **1966**, *5*, 232.
- (11) Fumagalli, P.; Schirmeisen, A. *J. Appl. Phys.* **1996**, *79* (8), 5929.
- (12) (a) Hao, X.; Moodera, J. S.; Meservey, R. *Phys. Rev. B* **1990**, *42* (13), 8235–8243. (b) Muller, C.; Lippitz, H.; Paggel, J. J.; Fumagalli, P. *J. Appl. Phys.* **2004**, *95* (11, Pt. 2), 7172–7174.
- (13) (a) Holtzberg, F.; McGuire, T. R.; Methfessel, S. *J. Appl. Phys.* **1966**, *37* (3), 976. (b) Holtzberg, F.; McGuire, T. R.; Methfessel, S.; Suits, J. C. *Phys. Rev. Lett.* **1964**, *13* (1), 18.
- (14) Schoenes, J.; Wachter, P. *Phys. Rev. B* **1974**, *9* (7), 3097.
- (15) Comment, A.; Ansermet, J.-P.; Slichter, C. P.; Rho, H.; Snow, C. S.; Cooper, S. L. *Phys. Rev. B* **2005**, *72*, 014428.
- (16) Ott, H.; Heise, S. J.; Sutart, R.; Hu, Z.; Chang, C. F.; Hsieh, H. H.; Lin, H. J.; Chen, C. T.; Tjeng, L. H. *Phys. Rev. B* **2006**, *73*, 094407.
- (17) Rho, H.; Snow, C. S.; Cooper, S. L.; Fisk, Z.; Comment, A.; Ansermet, J. *Ph. Int. J. Mod. Phys. B* **2002**, *16* (20–22), 3364.
- (18) (a) Arnold, M.; Kroha, J. *Phys. Rev. Lett.* **2008**, *100*, 046404. (b) Oliver, M. R.; Dimmock, J. O.; McWhorter, A. L.; Reed, T. B. *Phys. Rev. B* **1972**, *5* (3), 1078. (c) von Molnar, S.; Shafer, M. W. *J. Appl. Phys.* **1970**, *41* (3), 1093. (d) Ahn, K. Y.; McGuire, T. R. *J. Appl. Phys.* **1968**, *39* (11), 5061.
- (19) (a) Mauger, A.; Godart, C. *Phys. Rep.* **1986**, *141*, 51. (b) Mauger, A.; Escorne, M.; Godart, C.; Desfours, J. P.; Achard, J. C. *J. Physique Coll.* **1980**, *41*, C5265.
- (20) Mauger, A. *Phys. Status Solidi B* **1977**, *84*, 761.
- (21) (a) Arnold, M.; Kroha, J. *Phys. Rev. Lett.* **2008**, *100*, 046404. (b) Shapira, Y.; Foner, T.; Reed, S. B. *Phys. Rev. B* **1973**, *8*, 2299.
- (22) Von Molnar, S.; Methfessel, S. *J. Appl. Phys.* **1967**, *38* (3), 959.
- (23) Nowacki, W. *Z. Kristallogr.* **1938**, *99*, 339.
- (24) Jayaraman, A.; Bucher, E.; Dernier, P. D.; Longinotti, L. D. *Phys. Rev. Lett.* **1973**, *31* (11), 700.
- (25) Matsumoto, T.; Yamaguchi, K.; Yuri, M.; Kawaguchi, K.; Koshizaki, N.; Yamada, K. *J. Phys.: Condens. Matter* **2004**, *16*, 6017.
- (26) Mauger, A. *Phys. Status Solidi B* **1977**, *84*, 761.
- (27) Aharoni, A. *Introduction to the Theory of Ferromagnetism; International Series of Monographs on Physics 109*; Oxford University Press: Oxford, 2000; pp 80–82.
- (28) Wachter, P. In *Handbook on the Physics and Chemistry of Rare Earths*; Gschneidner, K. A., Eyring, L., Eds.; North-Holland Publishing Co.: 1979; Vol. 2, Chapter 19, pp 507–574.
- (29) Samokhvalov, A. A.; Arbuzova, T. I.; Simonova, M. I.; Fal'kovskaya, L. D. *Fizika Tv. Tela* **1973**, *15*, 3690.

JA104791X